Journal of Power Sources 242 (2013) 575–580

Contents lists available at SciVerse ScienceDirect

Journal of Power Sources

journal homepage: www.elsevier.com/locate/jpowsour

Amphiphilic block copolymer membrane for vanadium redox flow battery

Fei Wang*, James M. Sylvia, Monsy M. Jacob, Dharmasena Peramunage

EIC Laboratories, Inc., 111 Downey Street, Norwood, MA 02062, USA

HIGHLIGHTS

- Novel amphiphilic block copolymer was synthesized and membrane was developed.
- Improved vanadium ion selectivity and higher mechanical strength were demonstrated.
- Higher coulombic efficiency and energy efficiency comparable to Nafion were demonstrated.
- Much smaller capacity loss during 50 charge–discharge cycles was demonstrated.

ARTICLE INFO

Article history:
Received 15 March 2013
Received in revised form
2 May 2013
Accepted 21 May 2013
Available online 5 June 2013

Keywords:
Amphiphilic block copolymer
Proton exchange membrane
Vanadium redox flow battery
Energy storage

ABSTRACT

An amphiphilic block copolymer comprised of hydrophobic polyaryletherketone (PAEK) and hydrophilic sulfonated polyaryletherketone (SPAEK) blocks has been synthesized and characterized. A membrane prepared from the block copolymer is used as the separator in a single cell vanadium redox flow battery (VRB). The proton conductivity, mechanical property, VO^{2+} permeability and single VRB cell performance of this block copolymer membrane are investigated and compared to Nafion™ 117. The block copolymer membrane showed significantly improved vanadium ion selectivity, higher mechanical strength and lower conductivity than Nafion™ 117. The VRB containing the block copolymer membrane exhibits higher coulombic efficiency and similar energy efficiency compared to a VRB using Nafion™ 117. The better vanadium ion selectivity of the block copolymer membrane has led to a much smaller capacity loss during 50 charge–discharge cycles for the VRB.

1. Introduction

Vanadium redox flow batteries (VRB) hold great promise for large-scale electrochemical energy storage suitable for intermittent renewable energy sources like solar or wind [1–4]. A key component in the VRB is the ion exchange membrane separating the electrode compartments whose selectively allows cross-transport of non-active species (e.g., H^+, Na^+, etc.) to maintain electrical neutrality and electrolyte balance. Currently, the most commonly used ion exchange membranes for VRBs are made from perfluorinated copolymers such as Nafion™, which has high hydrolytic and oxidative stability and excellent proton conductivity. However, such perfluorinated polymers have the major drawback of very high cost and poor ionic selectivity. In the VRBs using perfluorinated membranes, the crossover of some active species has led to a loss of electrochemical energy during the operation [5]. To reduce cost and increase selectivity, extensive effort has been devoted to developing alternative non-perfluorinated polymer ion exchange membranes. Among the promising candidates are aromatic thermoplastic-based polymers such as polyaryletherketones, polyethersulfone, polyimide's, and polybenzimidazole [6,7]. These polymers have good chemical resistance, high thermo-oxidation stability, good mechanical properties, and are low cost. These polymers must be modified with ionic groups, typically sulfonate, in order to provide the required ionic conductivity [8–10]. To obtain a membrane material with high proton conductivity, the highest possible sulfonation level is desired. However, as the sulfonation level increases, the polymer becomes more hydrophilic, leading to enhanced swelling and lowering of its mechanical strength. Many investigations have been carried out using sulfonated aromatic polymers as membranes for VRB cell applications [11–14]. One potential problem of the non-perfluorinated sulfonated aromatic polymers is that it tends to be oxidatively damaged by the highly oxidizing pentavalent vanadium ion (VO_2^+) on the

* Corresponding author. Tel.: +1 781 769 9450; fax: +1 781 551 0283.
E-mail address: feiwang@eiclabs.com (F. Wang).

0378-7753/$ – see front matter © 2013 Published by Elsevier B.V.
http://dx.doi.org/10.1016/j.jpowsour.2013.05.102

positive electrode side of the cell, which makes them unable to offer long cycle life when used in the VRB system [11].

The use of amphiphilic block copolymer as membrane material offers a great potential. An important feature of this family of block copolymers is that they are expected to form an interpenetrating network (IPN) composed of highly hydrophobic unsulfonated regions, which contribute to the overall strong mechanical properties of the membrane, and highly hydrophilic sulfonated regions, which contribute to the high ionic conductivity of the membrane. Such phase separation is in some ways similar to the Nafion™ membrane, where hydrated sulfonate groups form conductive channels which contribute to the high ionic conductivity. There are reported studies involving the synthesis of amphiphilic block copolymers and their use as membrane materials for fuel cell applications [15–18]. They suggest that the block copolymer membrane architecture is superior to both random and alternating copolymer membrane systems under fuel cell operating conditions [18].

Here we report the synthesis of a novel amphiphilic block copolymer comprised of hydrophobic polyaryletherketone (PAEK) and hydrophilic sulfonated polyaryletherketone (SPAEK) blocks. A solvent-cast membrane prepared from this block copolymer is investigated for VRB applications. The proton conductivity, mechanical property, VO^{2+} permeability and single VRB cell performance of this block copolymer membrane are investigated and compared to Nafion™ 117. The block copolymer membrane showed significantly improved vanadium ion selectivity, higher mechanical strength and lower conductivity when compared to Nafion™ 117. The VRB assembled with block copolymer membrane exhibits higher coulombic efficiency and similar energy efficiency compared to a VRB using Nafion™ 117. The better vanadium ion selectivity of the block copolymer membrane has led to a much smaller capacity loss during 50 charge–discharge cycles for the VRB.

2. Experimental

2.1. Materials

4,4′-Difluorobenzophenone, anhydrous potassium carbonate, fuming sulfuric acid (20% SO_3), *N*,*N*-dimethylacetamide (DMAc) were obtained from Alfa Aesar, 4,4′-isopropylidenebis(2,6-dimethyl phenol) was obtained from Sigma–Aldrich. All other solvents and chemicals were obtained from Alfa Aesar and all chemical reagents were used as-received. Nafion™ 117 membrane and carbon felt were obtained from Alfa Aesar.

2.2. Block copolymer synthesis

The sodium sulfonated 4,4′-difluorobenzophenone monomer was synthesized following a reported procedure [19]. 4,4′-Difluorobenzophenone was sulfonated using fuming sulfuric acid (20% SO_3) which was followed by neutralization to produce the monomer for polymer synthesis. The sodium sulfonated 4,4′-difluorobenzophenone was further purified by Soxhlet extraction using ethanol as solvent.

The block copolymer synthesis was carried out as shown in Fig. 1. The synthesis of polyaryletherketone (PAEK) was carried out by reaction of 4,4′-difluorobenzophenone (2.18 g, 10 mmol) with 4,4′-isopropylidenebis(2,6-dimethylphenol) (2.56 g, 9 mmol) in 30 mL DMAc and K_2CO_3 (1.37 g, 9.9 mmol) in a three-neck flask equipped with magnetic stirring. Toluene, 15 mL was added to the mixture and the reaction flask was heated to 165 °C with oil bath. The Dean–Stark distillation head was used with refluxing toluene to dry the reaction mixture for 40 min and then the temperature was raised to 180 °C to remove all toluene. The polymerization reaction was continued at 180 °C for 48 h. The mixture, after cooling was poured into acetone to precipitate the PAEK polymer product. After repeated washing with acetone and dried under vacuum, 3.99 g of PAEK polymer was obtained (96% yield).

The synthesis of sulfonated polyaryletherketone (SPAEK) was carried out by the reaction of sodium sulfonated 4,4′-difluorobenzophenone (3.80 g, 9 mmol) with 4,4′-isopropylidenebis(2,6-dimethylphenol) (2.84 g, 10 mmol) in 30 mL DMAc and K_2CO_3 (1.37 g, 9.9 mmol) using the same procedure as for PAEK. The SPAEK polymer was precipitated by pour into 2-propanol of the cooled reaction mixture and the product was cleaned by washing repeatedly with 2-propanol. After drying in vacuum, 5.09 g of SPAEK polymer was obtained (85% yield).

The synthesis of block copolymer poly(sulfonated polyaryletherketone-*b*-polyaryletherketone) (PSP) was carried out by the reaction of PAEK (3.79 g, 8 mmol repeat unit weight) with SPAEK (3.53 g, 5.3 mmol repeat unit weight) in 30 mL DMAc and K_2CO_3 (1.10 g, 8 mmol) using the same procedure as for SPAEK. Block copolymer PSP was obtained in 75% yield (5.49 g). The sodium sulfonate group ($-SO_3Na$) in PSP was converted to sulfonic acid group ($-SO_3H$) by stirring the polymer powder with 10% HCl at 100 °C for 1 h followed by washing with water and drying at vacuum.

Size exclusion chromatography (SEC) was used to determine the molecular weights, only SPAEK is soluble at room temperature for SEC analysis. SEC measurements were conducted using a Hewlett–

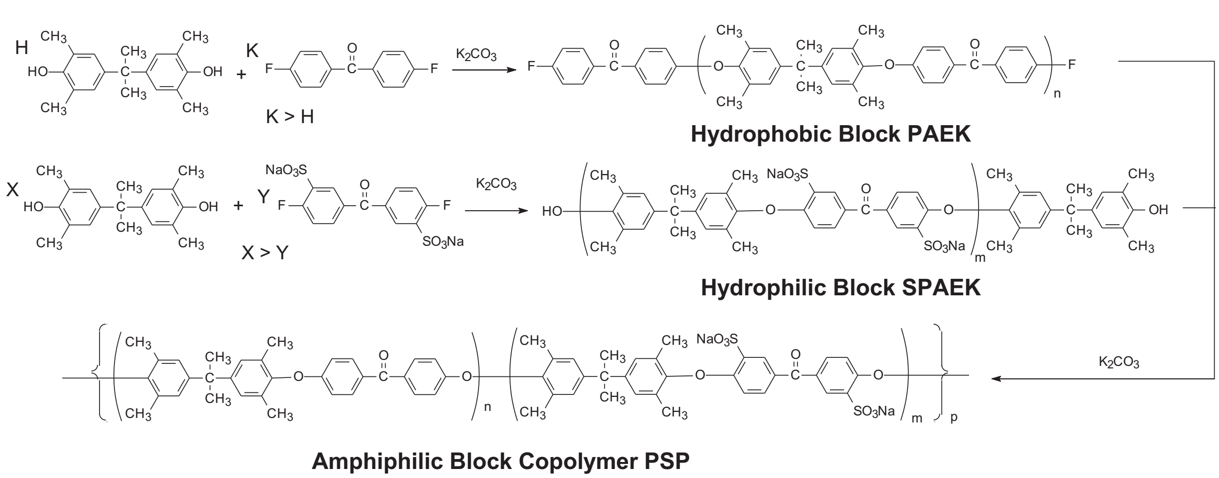

Fig. 1. Scheme for the synthesis of poly(SPAEK–PAEK) block copolymer (PSP) via a two-pot reaction.

Packard series 1050 HPLC equipped with a Polymer Laboratories PL gel 5 μ mixed-D column and a Hewlett–Packard 1047A refractive index detector. DMAc was used as the eluting solvent at a flow rate of 0.5 mL min^{-1} while maintaining the column at 35 °C. Polystyrene standard samples were used to calculate relative molecular weight of SPAEK.

2.3. Casting of the membrane

The PSP polymer was dissolved in DMAc by stirring at 150 °C for 30 min to make 10% wt. polymer solution. The solution was cast into a leveled glass plate on a hot plate heated to 100 °C followed by drying at 90 °C for 10 min to remove most of the solvent, and then drying slowly at 80 °C for 2 h. The thickness of the resulting PSP membrane was 70–80 μm.

2.4. Membrane properties

The mechanical strength of the membranes was measured by tensile testing on an Instron 4204 Electromechanical Test System. The water-saturated membranes were cut into "dog-bone"-shaped specimens and mounted on the tensile test machine. The load was 100 lb at 0.5 inch min^{-1} speed.

The ion exchange capacity (IEC) values of membranes were determined using a simple titration method. Membranes weighing about 0.1 g were soaked in 1 M HCl aqueous solution for 24 h to convert them completely into the H-form. Then the membranes were soaked and washed with deionized water over 8 h to remove all free acid. The membranes were equilibrated with 25.0 mL of 0.01 M NaOH solution in a tightly capped volumetric flask. After a 16 h soak, the alkaline solutions were titrated with 0.01 HCl until pH 7 was reached using a pH meter. Equivalents of NaOH consumed by the membrane were determined by difference relative to the baseline titration without the membrane.

The membrane surface conductivities were measured by the 4-probe method as reported in the literature [20] using electrochemical impedance spectroscopy. The membrane area resistance was determined in the VRB cell filled on both sides with 0.5 M $VOSO_4$ in 3 M H_2SO_4 using impedance spectroscopy. The calculation was carried out using the equation: $r = (r_1 - r_2)S$, where the cell resistance (r_1) measured when membrane was inside the cell and (r_2) is cell resistance without membrane, S is the area of the membrane exposed to the electrolyte.

2.5. Permeability of VO^{2+}

The permeability of vanadium ions through the membrane was measured using the VRB cell. The membrane mounted in the cell was exposed to a solution of 1.5 M $VOSO_4$ in 3 M H_2SO_4 on the left side and a solution of 1.5 M $MgSO_4$ in 3 M H_2SO_4 on the right side. $MgSO_4$ was used to equalize the ionic strengths of the two solutions and to minimize the osmotic effects. Either solution was circulated through the cell compartments separated by the membrane using peristaltic pumps. The effective area of the exposed membrane was 5 cm^2 while the volumes of the solutions for each reservoir were 50 mL. Samples of solution from the right reservoir were taken at regular time intervals and analyzed for vanadium ion concentration using UV–vis spectroscopy.

2.6. VRB cell performance

The carbon felt (0.5″ thickness) was used as electrodes; the compression was 40%. Graphite plates (composite graphite bipolar plate, Graphitestore.com) were used as the current collectors. The electrolyte solution reservoirs were made from Kel-F (polychlorotrifluoroethylene, PCTFE), and the volume was about 50 mL. They were capped with rubber stoppers, and argon gas was flowed over active solutions in the reservoirs to protect them from air oxidation. The tubes connecting the reservoirs to the cell were made of Viton. The VO_2^+/VO^{2+} and V^{3+}/V^{2+} solutions were pumped from the electrolyte solution reservoirs through each cell chamber at ~20 mL min^{-1} using separate peristaltic pumps (model SP202V1R.406, APT Instruments). The membrane working area was 5 cm^2. The charge/discharge cycling of the cell was carried out between 1.7 V and 0.8 V using a Gamry Electrochemical Measurement System (Model Reference 600 Potentiostat/Galvanostat/ZRA, Gamry Instruments). The PWR800™ Electrochemical Energy Software (Gamry) was used to operate the system and to record data. The chosen cell cycling limits are consistent with those used in the reported investigations [13,14].

The electrolyte used in the VRB cell was prepared by dissolving $VOSO_4$.3.5 H_2O (Alfa Aesar) in 3 M H_2SO_4, affording a 1.5 M $VOSO_4$ solution. The same $VOSO_4$ solution was used on both sides of the VRB cell reservoirs with twice as much electrolyte volume in the anode compartment as that was used in the cathode compartment. The electrochemical oxidation/reduction was carried out until all the VO^{2+} in the anode was oxidized to VO_2^+, and all the VO^{2+} in the cathode have reduced to V^{2+}. Then half of the anode solution was removed, leaving a balanced VO_2^+ and V^{2+} electrolyte in the system for the cycling study. A fresh electrolyte solution was used for each experiment involving charge/discharge cycling. While due attention was paid to maintain a balanced capacity in the two compartments of the cell, no attempts were made to maintain uniform capacities among different runs.

3. Results and discussion

3.1. Block copolymer synthesis

The block copolymer of PSP was synthesized following the scheme shown in Fig. 1. The hydrophobic polymer PAEK and the hydrophilic polymer SPAEK were synthesized separately. The monomer feed ratio was controlled to be in imbalance so that the polymer length would be relatively short with desired terminal functional groups. For example, the synthesis of PAEK polymer was carried out with K = 10 and H = 9 so that the PAEK polymer will have fluorine as the terminal group. Likewise, with X = 10 and Y = 9 the SPAEK polymer will end up with hydroxyl groups at both terminals. The synthesis of block copolymer PSP was carried out using excess PAEK polymer so that the final block copolymer has a desired overall hydrophobic/hydrophilic ratio of 1.5 and the resulting copolymer will have PAEK blocks at both ends of the polymer chain.

The SPAEK polymer is soluble in DMAc at room temperature so that it can be characterized by SEC for its molecular weight. In contrast, as PAEK and PSP polymers are soluble in DMAc only at elevated temperatures (>100 °C), their characterization by SEC is not feasible. The SEC analysis for SPAEK polymer using the polystyrene standard showed relative molecular weights of $M_w = 114$ K and $M_n = 39$ K. Since the monomer feed ratio for the synthesis of PAEK is similar to that for SPAEK, the polymer chain length should be similar. The molecular weight of PSP copolymer is unknown. The structure of the PAEK, SPAEK, and PSP copolymers were confirmed by IR spectroscopy. The PAEK polymer showed no –OH bands while the characteristics bands for entire polymer backbone were clearly identifiable. The SPAEK polymer is hydroxyl terminated and the IR spectrum showed all the PAEK bands together with those for –OH and $-SO_3Na$ located at 3446, 1309 and 1166 cm^{-1}. IR spectra for the PSP copolymers showed a combination of the two constituent blocks. The $-SO_3Na$ had converted to $-SO_3H$ and its corresponding

Table 1
Mechanical properties of PSP and Nafion™ membranes.

	Young's modulus (MPa)	Tensile strength (MPa)	Elongation at break (%)
PSP	205.2	48.6	53
Nafion™	20.5	10.4	122

bands shifted slightly to 3438, 1307, 1157 cm^{-1} ($-SO_3H$). The two bands located at 1027 and 1081 cm^{-1} representative of S=O are not present in the PAEK IR spectrum but are present in both spectra for the SPAEK and the copolymer based on it.

3.2. Membrane characterization

3.2.1. Mechanical property

The mechanical properties of the water-saturated PSP membrane and Nafion™ membrane are characterized by Tensile testing and the results are summarized in Table 1. The PSP membrane appeared much stiffer than Nafion™. The stress, in this case, increased more rapidly with the applied load. The Nafion™ membrane was softer and showed a more elastic property with elongation initially followed by increasing stress with load. The Young's modulus of the PSP membrane is almost ten times that for Nafion™, demonstrating high mechanical strength, which is highly desirable and suggesting that thinner membranes could be developed with acceptable mechanical properties.

3.2.2. Membrane property characterization

The membrane properties are summarized in Table 2. The PSP membrane has lower water uptake and IEC than that of Nafion™. The surface conductivity measured by the 4-probe method is lower for the PSP membrane. The membrane area resistance measured by in VRB cell showed the cross-membrane resistance is higher for the PSP as well.

3.2.3. Permeability of VO^{2+}

As a result of the permeation through the membrane, the VO^{2+} ion concentration increases in the $MgSO_4$ compartment as shown in Fig. 2. The VO^{2+} permeability was calculated following the literature reported method [21] assuming the permeability (P) is independent of VO^{2+} concentration. The P values for Nafion™ and PSP were 2.77×10^{-7} cm^2 min^{-1}, and 1.37×10^{-8} cm^2 min^{-1} respectively, clearly indicating that PSP membrane is much superior to Nafion™ in terms of its selectively for the VO^{2+} ion.

3.3. VRB cell performance evaluation

3.3.1. Open circuit voltage measurements

The vanadium ions leakage through the membrane in the VRB cell was identified as the main reason for the observed cell capacity losses. Open circuit voltage (OCV) measurements are often used as an indirect method to compare the ion selectivity and permeability of different membranes. The VRB cells using a Nafion™ membrane and a PSP membrane were fully charged, and the OCVs were measured while the electrolyte solutions were continually pumped

Table 2
Membrane properties.

	Water uptake (%)	IEC (mmol g^{-1})	Conductivity (S cm^{-1}, 4-probe method)	Area resistance (Ω cm^2)
PSP	7.8	0.74	4.9×10^{-2}	1.5
Nafion™	14.0	0.94	1.04×10^{-1}	0.8

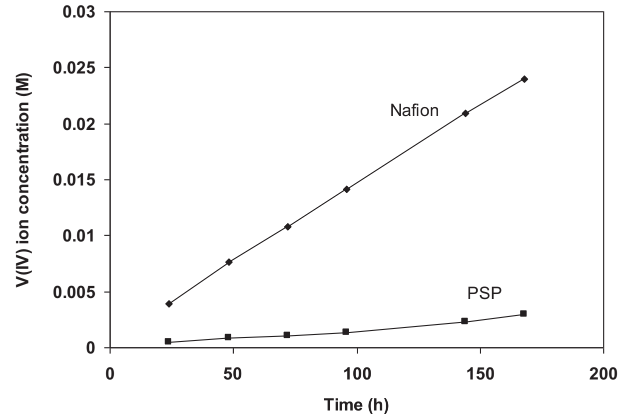

Fig. 2. Increase in the concentration of VO^{2+} in the $MgSO_4$ compartment as a result of permeation trough the PSP and Nafion™ membranes.

through the cell. As showed in Fig. 3, the OCV of the VRB cell with the Nafion™ membrane gradually decreased from 1.47 V with time at first, and then dropped rapidly in about 66 h to 0.8 V, and then continued decaying to 0.74 V in 100 h. However, the VRB cell using the PSP membrane held the OCV fairly well up to 100 h without showing a sharp drop. The OCV changed only a modest amount from $V_0 = 1.50$ V to $V_{100} = 1.45$ V. The results demonstrated that the PSP membrane has lower vanadium ion permeability, leading to a much longer charge retention capability than Nafion™ in a VRB cell. The self-discharge that leads to a sharp drop in the OCV is a common phenomenon in VRB cells. The reason has been attributed to the leakage of vanadium ions through the membrane causing some reactions between the vanadium ions at different oxidation states [11]. Experimental and theoretical investigations have indicated that the diffusion of vanadium ions through a membrane, caused by the difference in the concentration of vanadium ions in the positive and negative compartments, as the main reason for this crossover [21–23].

3.3.2. VRB cell cyclic studies

We evaluated the charge/discharge cycling performance of a VRB single cell using the Nafion™ membrane. The electrolyte solution consisted of 0.5 M each VO^{2+} and V^{3+} in 3 M H_2SO_4 and the charge and discharge cycling was carried out galvanostatically at 20 mA cm^{-2} using 1.7 V and 0.8 V as charge and discharge cutoffs respectively. Shown in Fig. 4 are the capacity vs. voltage profiles for

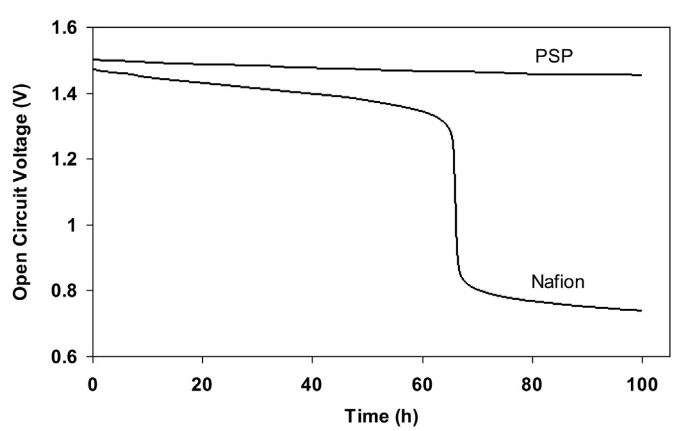

Fig. 3. Open circuit voltage decay of fully charged VRB cell with PSP and Nafion™ membranes.

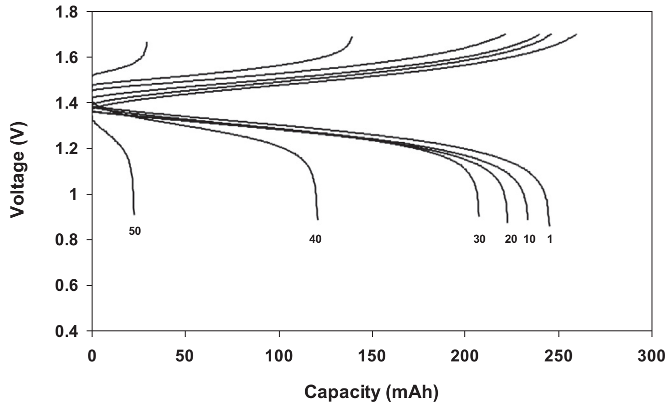

Fig. 4. The charge–discharge curves for a VRB cell containing the Nafion™ membrane over 50 cycles.

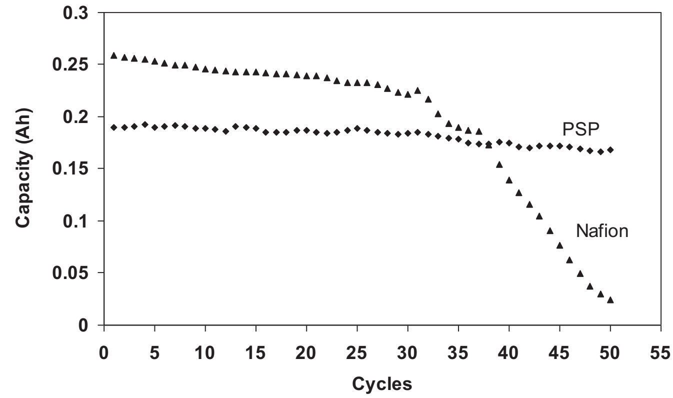

Fig. 6. Capacity changes of VRB with Nafion™ and PSP membrane over 50 cycles.

a selected number of cycle's for a VRB cell with a Nafion™ membrane that underwent over 50 charge/discharge cycles. It can be seen that the charge–discharge capacity of the cell has reduced relative rapidly over the 50 cycles with a concomitant shift of the starting position of each charge-discharge cycle in the anodic and cathodic direction respectively. The ions leakage through the Nafion™ membrane could be the main reason for this observed loss of capacity.

The capacity vs. voltage characteristics of a VRB cell observed during the extended charge–discharge cycling of a VRB cell with the PSP membrane are shown in Fig. 5. The experimental conditions were the same as for the VRB cell with the Nafion™ membrane. Due to the higher membrane resistance, the voltage gap between the starting positions of each charge–discharge cycle was higher. However, the voltage gap remained almost constant over the 50 cycles. The capacity loss over the 50 cycles was relatively small compared to that for the cell with the Nafion™ membrane, suggesting that the permeability of active vanadium ionic species across the PSP membrane is taking place at a much lower rate than for the cell containing the Nafion™ membrane.

A comparison of the discharge capacity as a function of cycle number for VRB cells containing either Nafion™ or the PSP membrane is shown in Fig. 6. The initial capacity of the cell containing the PSP membrane was lower compared to Nafion. This may be due to batch to batch inconsistencies in electrolyte concentrations. Both cells showed a capacity decline with cycling although, it is much less pronounced for the cell with the PSP membrane. The same cell showed a significantly better cycle life as well. The average capacity loss per cycle for the cell with Nafion™ membrane was 4.7 mAh per cycle whereas it was just 0.42 mAh per cycle for the cell with the PSP membrane.

The coulombic and energy efficiency performance of the cells are plotted in Fig. 7. The coulombic efficiencies for the cell with the PSP membranes are higher throughout the cycling due to the better ion selectivity. The voltage efficiencies of the PSP membrane are lower due to a higher resistance than that for Nafion™. The combined overall energy efficiency was slightly lower for the cell with the PSP membrane. It was very encouraging to observe that the PSP membrane showed no visual evidence for any degradation after remaining in the cell for over 50 cycles.

Generally, compared to perfluorinated materials like Nafion™, membranes made from hydrocarbon materials are less stable, particularly in VRB cells where strong acidic conditions and strong oxidative of VO_2^+ are present, causing the membrane to degrade during the repeated cycling [11]. The membrane made from the block copolymer PSP appeared to remain very stable in VRB under these harsh conditions. The PSP membrane did not show any visual degradation after a 50-cycle run and the same membrane showed virtually the same performance in subsequent cycling in the same electrolyte. The stability could be attributed to the unique structure of the PSP copolymer. The weak part in the polyaryletherketone polymer backbone is the ether linkage which can be attacked by strong acid leading to degradation of the membrane. In the PSP copolymer, all ether linkages are located in the vicinity of phenyl groups carrying two methyl groups. Such steric crowding could

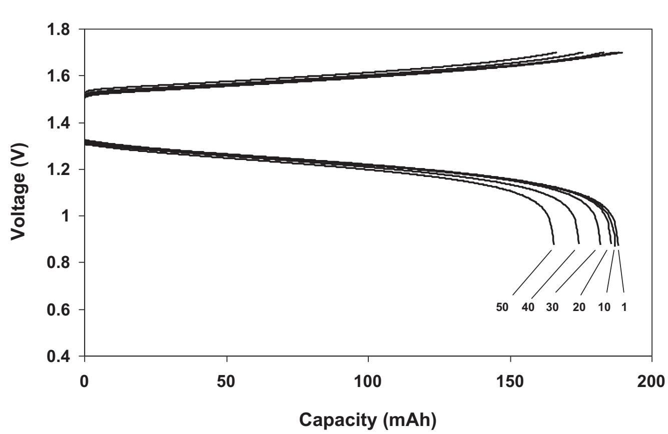

Fig. 5. The charge–discharge curves for a VRB cell containing the PSP membrane over 50 cycles.

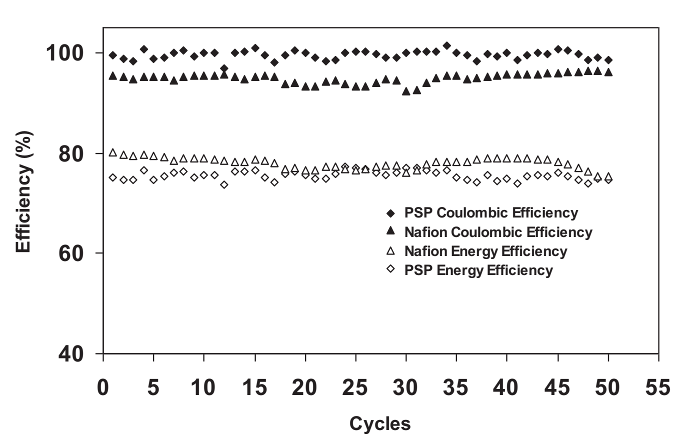

Fig. 7. VRB cell performance comparison.

protect the ether linkage reducing its susceptibility to acid and also, minimizing the oxidation of the polymer chain.

4. Conclusions

In this study, amphiphilic block copolymer PSP with hydrophobic PAEK and hydrophilic SPAEK blocks was synthesized and characterized. The membrane prepared from PSP copolymer was investigated for VRB applications. The membrane properties were evaluated and compared with Nafion™ 117. The PSP membrane showed lower conductivity but higher mechanical strength than Nafion™. PSP membrane also showed significantly improved vanadium ion selectivity and that lead to very stable OCV due to less vanadium ions loss via crossover through the membrane. The VRB containing a PSP membrane exhibited higher coulombic efficiency similar energy efficiency compared to a VRB using Nafion™ 117. Better vanadium ion selectivity of the PSP membrane has led to much smaller capacity loss during charge–discharge cycling for over 50 cycles. The results demonstrated a pronounced stability of the PSP membrane towards the harsh conditions prevailing in a VRB cell. The material cost for the membrane is approximately $100 per square meter which is much cheaper than Nafion 117. Expanded investigation including a scaled-up fabrication of the membrane is currently underway.

Acknowledgments

Funding of this work by the DOE (DE-SC0004382) is gratefully acknowledged. The authors thank Dr. Michael D. Gilbert for help in evaluating membrane mechanical properties and Dr. R. David Rauh for his helpful discussions during this work.

References

[1] C. Ponce de Leon, A. Frias-Ferrer, J. Gonzalez-Garcia, D.A. Szanto, F.C. Walsh, J. Power Sources 160 (2006) 716.
[2] T. Mohammadi, M. Skyllas-Kazacos, J. Membr. Sci. 107 (1995) 35.
[3] Z. Yang, J. Zhang, M.C.W. Kintner-Meyer, X. Lu, D. Choi, J.P. Lemmon, J. Liu, Chem. Rev. 111 (2011) 3577.
[4] W. Wang, Q. Luo, B. Li, X. Wei, L. Li, Z. Yang, Adv. Funct. Mater. (2012), http://dx.doi.org/10.1002/adfm.201200694.
[5] X. Luo, Z. Lu, J. Phys. Chem. B 109 (2005) 20310.
[6] M.A. Hickner, H. Ghassemi, Y.S. Kim, B.R. Einsla, J.E. McGrath, Chem. Rev. 104 (2004) 4587.
[7] D.J. Jones, J. Roziere, J. Membr. Sci. 185 (2001) 41.
[8] A.L. Rusanov, D. Likhatchev, P.V. Kostoglodov, K. Mullen, M. Klapper, Adv. Polym. Sci. 179 (2005) 83.
[9] D.Y. Chen, S.J. Wang, M. Xiao, Y.Z. Meng, Energy Environ. Sci. 3 (2010) 622.
[10] K. Miyatake, T. Shimura, T. Mikami, M. Watanabe, Chem. Commun. (2009) 6403.
[11] S. Kim, J. Yan, B. Schwenzer, J. Zhang, L. Li, J. Liu, Z. Yang, M.A. Hickner, Electrochem. Commun. 12 (2010) 1650.
[12] D. Chen, S. Wang, M. Xiao, Y. Meng, J. Power Sources 195 (2010) 2089.
[13] Z. Mai, H. Zhang, X. Li, C. Bi, H. Dai, J. Power Sources 196 (2011) 482.
[14] W. Wei, H. Zhang, X. Li, Z. Mai, H. Zhang, J. Power Sources 208 (2012) 421.
[15] A. Roy, H.-S. Lee, J.E. McGrath, Polymer 49 (2008) 5037.
[16] B. Bae, T. Hoshi, K. Miyatake, M. Watanabe, Macromolecules 44 (2011) 3884.
[17] C.K. Shin, G. Maier, B. Andreaus, G.G. Scherer, J. Membr. Sci. 245 (2004) 147.
[18] M.L. Einsla, Y.S. Kim, M. Hawley, H. Lee, J.E. McGrath, B. Liu, M.D. Guiver, B.S. Pivovar, Chem. Mater. 20 (2008) 5636.
[19] F. Wang, T. Chen, J. Xu, Macromol. Chem. Phys. 199 (1998) 1421.
[20] C.H. Fujimoto, M.A. Hickner, C.J. Cornelius, D.A. Loy, Macromolecules 38 (2005) 5010.
[21] C. Sun, J. Chen, H. Zhang, X. Han, Q. Luo, J. Power Sources 195 (2010) 890.
[22] E. Wiedemann, A. Heintz, R.N. Lichtenthaler, J. Membr. Sci. 141 (1998) 215.
[23] D. You, H. Zhang, C. Sun, X. Ma, J. Power Sources 196 (2011) 1578.